

This article was downloaded by:

On: 25 January 2011

Access details: *Access Details: Free Access*

Publisher *Taylor & Francis*

Informa Ltd Registered in England and Wales Registered Number: 1072954 Registered office: Mortimer House, 37-41 Mortimer Street, London W1T 3JH, UK



Liquid Crystals

Publication details, including instructions for authors and subscription information:

<http://www.informaworld.com/smpp/title~content=t713926090>

Antiferroelectric siloxane liquid crystal dimers with large molecular tilt under an applied electric field

Nils Olsson^a; Gunnar Andersson^b; Bertil Helgee^a; Lachezar Komitov^b

^a Polymer Technology, Department of Chemical and Biological Engineering, Chalmers University of Technology, Göteborg, Sweden ^b Liquid Crystal Physics, Department of Physics, Gothenburg University, Gothenburg, Sweden

To cite this Article Olsson, Nils , Andersson, Gunnar , Helgee, Bertil and Komitov, Lachezar(2005) 'Antiferroelectric siloxane liquid crystal dimers with large molecular tilt under an applied electric field', *Liquid Crystals*, 32: 9, 1125 – 1138

To link to this Article: DOI: 10.1080/02678290500268135

URL: <http://dx.doi.org/10.1080/02678290500268135>

PLEASE SCROLL DOWN FOR ARTICLE

Full terms and conditions of use: <http://www.informaworld.com/terms-and-conditions-of-access.pdf>

This article may be used for research, teaching and private study purposes. Any substantial or systematic reproduction, re-distribution, re-selling, loan or sub-licensing, systematic supply or distribution in any form to anyone is expressly forbidden.

The publisher does not give any warranty express or implied or make any representation that the contents will be complete or accurate or up to date. The accuracy of any instructions, formulae and drug doses should be independently verified with primary sources. The publisher shall not be liable for any loss, actions, claims, proceedings, demand or costs or damages whatsoever or howsoever caused arising directly or indirectly in connection with or arising out of the use of this material.

Antiferroelectric siloxane liquid crystal dimers with large molecular tilt under an applied electric field

NILS OLSSON[†], GUNNAR ANDERSSON[‡], BERTIL HELGEE[†] and LACHEZAR KOMITOV^{*‡}

[†]Polymer Technology, Department of Chemical and Biological Engineering, Chalmers University of Technology, Kemivägen 4 SE-412 96, Göteborg, Sweden

[‡]Liquid Crystal Physics, Department of Physics, Gothenburg University, SE-412 96, Gothenburg, Sweden

(Received 9 March 2005; accepted 27 June 2005)

The scope of the present study is the response of a series of antiferroelectric dimeric or bimesogenic siloxanes to an applied electric field with focus on their pretransitional behaviour and the field-induced antiferro–ferroelectric (AF–F) transition. Most of these compounds possess a molecular tilt close to 45° and spontaneous polarization in the field-induced ferroelectric (F) phase in the range of 250–300 nC cm⁻². In the dimers with a spacer length exceeding five carbons, a transformation from first to second order of the field-induced AF–F transition is found with temperature. Several different indications for this transformation are identified and their characteristics are discussed in the framework of the existing theoretical models. A large field-induced in-plane deviation of the sample optic axis was observed in the pretransitional region of several of the siloxane dimers and is likely due to the flexibility of the linking chains. The potential of the antiferroelectric bimesogenic siloxanes for displaying high contrast images and grey scale capability is shortly discussed. The large molecular tilt close to 45° in combination with the field-induced AF–F transition of second order seems to be the most attractive features of these materials.

1. Introduction

The molecules of smectic liquid crystals are arranged into layers, i.e. they have a positional order, forming two-dimensional liquids. In addition to the positional order, the molecules of tilted smectics are oriented at a fixed angle θ (tilt angle) with respect to the layer normal. If the constituent molecules of the tilted smectics are chiral and the molecular tilt in each smectic layer has the same sign, i.e. the molecules possess synclinc order, each smectic layer exhibits a spontaneous polarization \mathbf{P}_s directed perpendicular to the molecular tilt plane that includes the smectic layer normal and the long molecular axis. The chiral tilted smectic liquid crystals with synclinc molecular order form the class of ferroelectric liquid crystals (FLCs). Antiferroelectric liquid crystals (AFLCs) belong to the general class of tilted chiral smectic liquid crystals in which the molecular tilt angle in the adjacent smectic layers has opposite sign, i.e. they possess anticlinc order. In the AFLC, the c -director (the projection of the long molecular axis onto the smectic layer plane) of adjacent layers is almost antiparallel. As a result of the anticlinc molecular order, the \mathbf{P}_s vectors in the adjacent

smectic layers of the AFLCs are nearly antiparallel. Hence, the AFLCs do not exhibit a spontaneous polarization due to the anticlinc molecular order. An external electric field of certain strength applied along the smectic layers of the AFLC, however, may align the \mathbf{P}_s of each smectic layer along the electric field and, hence, induce an F state. This field-induced F state was first reported by Chandani *et al.* [1, 2] and soon became of great scientific and technological interest. The field-induced AF–F transition can be of first or second order depending on the height of the energy barrier between AF and F states [3]. A very specific feature of the field-induced AF–F transition of first order is the generation of quasi-one-dimensional finger-like solitary waves propagating along the smectic layers analogous to the solitary waves observed in short pitch FLCs [4]. The first-order AF–F transition is preceded by a more or less pronounced pretransitional effect broadly discussed in the literature [3, 5–8]. In this article we report investigations on the field-induced AF–F transition and the pretransitional behaviour of a series of bimesogenic siloxanes. Some of these compounds possessed a broad temperature AF phase and/or large molecular tilt close to 45°. One of the compounds, di(4PPB6)3Si, with medium length chains connecting the mesogens in dimers were found at low temperature to exhibit a

*Corresponding author. Email: komitov@fy.chalmers.se

field-induced AF–F transition of second order; the compound with the longest chain showed similar tendencies but crystallized before the transformation of the AF–F transition from first to second order was completed.

2. Experimental

2.1. Materials

The synthesis of the dimeric siloxane liquid crystals studied in this work has been described in detail in another paper [9]. The general structure of these materials is shown together with their phase sequences in table 1. The designation of these materials in the present work is di(4PPB m)3Si, where m is the number of C-atoms in the chain connecting the siloxane group with the mesogens. As is shown in the table, they all exhibit an antiferroelectric phase which for some of the compounds exists over a broad temperature interval. It should be pointed out that none of the monomers corresponding to these dimers shows an AF phase.

2.2. Characterization

Optical and electro-optical characterization of the bimesogenic siloxane materials was performed in a set-up consisting of a polarizing microscope with camera, photodetector and function generator with amplifier and oscilloscope. The polarizing microscope was equipped with a Mettler FP52 hot stage and FP5 control unit ensuring temperature accuracy within $\pm 0.1^\circ\text{C}$. A Diamant bridge was used to measure the spontaneous polarization [10].

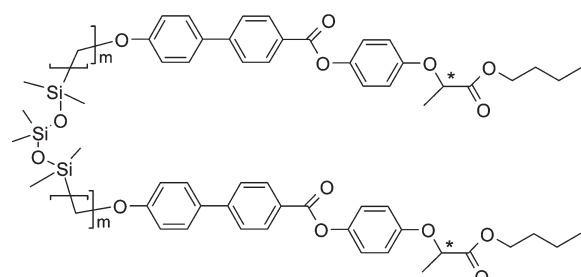
2.3. Sample preparation

Electro-optical studies were carried out on commercially available sandwich cells for evaluation of liquid crystals (purchased from E.H.C. Co. Ltd, Japan). The alignment layer in these cells favoured bookshelf alignment (with smectic layers lying perpendicular to the cell substrates) of the liquid crystal material filling the cell. Cells with gap of 2 or 4 μm were filled with the liquid crystal material in the isotropic phase by capillary forces. The uniformity of the bookshelf alignment was substantially improved by switching the sample in the F state for some time at high temperatures. In some cases, cells with bookshelf texture possessing a random in-plane preferred direction of alignment were used in our evaluation. Such samples possessed alignment with a polydomain texture that consisted of circular and/or focal-conic domains.

3. Theoretical background

The behaviour of bi-mesogenic siloxanes under an applied electric field was studied. The experimental results obtained are discussed in the frame of existing theoretical models presented in brief below. In general, in AFLCs, a helical molecular order is imposed on the *antclinic* order. For the sake of simplicity, such a helical order will be excluded from further discussion. In fact, the helix of an AFLC can be suppressed effectively by the liquid crystal interactions with the surface of the confining substrates in the same manner as in the case of an unwound FLC. The free energy of an unwound AFLC layer with thickness d , according to the geometry

Table 1. The general structure of the bimesogenic siloxanes, di(4PPB m)3Si, studied in this work and their phase sequences. Di(4PPB3)3Si and di(4PPB4)3Si possess only a monotropic AF phase, therefore their transition temperatures are given on cooling.



Compound	Treatment	m	Transition temperatures/ $^\circ\text{C}$			
di(4PPB3)3Si	heating	3	Cr 79	I		
di(4PPB3)3Si	cooling	3	X 33	SmC _A 59	I	
di(4PPB4)3Si	cooling	4	X < 25	SmC _A 68	I	
di(4PPB5)3Si	heating	5	X 76	SmC _A 91	I	
di(4PPB6)3Si	heating	6	X 17	SmC _A 90	SmC* 96	I
di(4PPB11)3Si	heating	11	X 30	SmC _A 108	SmA* 122	I

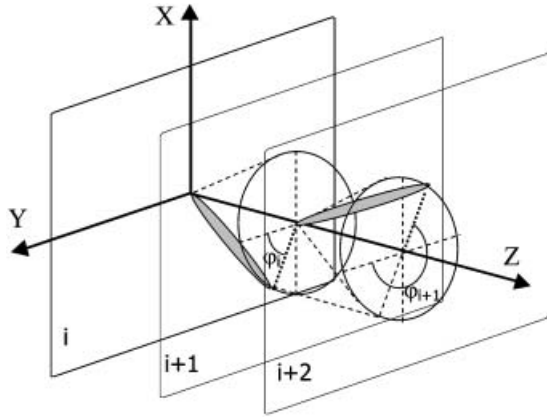


Figure 1. Geometry of the theoretical model of an AFLC. φ_i is the azimuthal angle that the projection of the director \mathbf{n} in the i -layer onto the XY -plane makes with the Y -axis. In field-free conditions the azimuthal angles in two adjacent layers obey the condition $\varphi_{i+1} - \varphi_i = \pi$.

of the model AFLC given in figure 1, reads [3]:

$$F = d \sum_i \int f_i dx dy$$

where f_i is the free energy of the i_{th} smectic layer given by:

$$f_i = \frac{1}{2} K \sin^2 \theta \left[\left(\frac{\partial \varphi_i}{\partial x} \right)^2 + \left(\frac{\partial \varphi_i}{\partial y} \right)^2 \right] - \mathbf{P}_o \cdot \mathbf{E} \cos \varphi_i + U \cos(\varphi_{i+1} - \varphi_i) - \frac{J}{2} \cos[2(\varphi_{i+1} - \varphi_i)] \quad (1)$$

where θ is the molecular tilt; φ_i is the azimuthal angle that the projection of the director \mathbf{n} in the i -layer onto the XY -plane makes with the Y -axis; \mathbf{P}_o is the polarization within the i -layer lying perpendicular to the molecular tilt plane. K is an average elastic constant, U represents the coupling coefficient that favours the AF ordering, while J represents the energy barrier between AF and F ordering, i.e. between *antclinic* and *synclinic* ordering. In an undistorted AF state the azimuthal angles in two adjacent layers obey the condition $\Delta\varphi = \varphi_{i+1} - \varphi_i = \pi$. The third and fourth terms in equation (1) represent the dipolar and quadrupolar interlayer interactions, respectively. These interactions are still not well understood; they are considered to be a combination of steric and electrostatic forces. The character of the interlayer interactions determines whether the molecules will adopt synclinic or anticlinic order. It should be noted here that, in our case, the siloxane group bridging two symmetric mesogenic parts of the molecules in a dimeric structure resulted in an anticlinic order of the mesogens, i.e. the so-called conformational antiferroelectricity [11].

For a sufficiently high energy barrier J , the field-induced AF–F transition is of first order, manifested by generation and propagation of quasi-one-dimensional finger-like solitary waves along the smectic layers [4], while a low energy barrier J will result in a second order AF–F transition with an almost continuous transition from AF to F ordering, i.e. a thresholdless AF–F transition. In figure 2, a sequence of photomicrographs illustrates typical textural changes due to the field-induced AF–F transition found in most of the dimeric siloxanes studied in this work.

In a simplified model [4] in which J is neglected, the field strength at which the AF–F transition takes place is given by:

$$\mathbf{E}_{th}^{AF-F} = \frac{2U}{\mathbf{P}_s} \quad (2)$$

where \mathbf{P}_s is the spontaneous polarization of the field-induced F state. As seen, in this model, \mathbf{E}_{th}^{AF-F} is independent of cell thickness. After the applied electric field is switched off, the AF state emerges from the F state. The relaxation time τ_r of the AF state is an important characteristic of the switching process in AFLCs. $\tau_r = 1/v_r$, where v_r is the velocity of retreating fingers of the recovering AF state [4]:

$$v_r = \frac{2}{\gamma} (2UK \sin^2 \theta)^{1/2} \propto \frac{U^{1/2}}{\gamma_n} \quad (3)$$

where γ is the rotational viscosity. Then, from equation (3) it follows that $\tau_r = 1/v_r \sim \gamma_n/U^{1/2}$, where $\gamma_n^2 = \gamma^2/K$ (normalized viscosity).

Several authors [3, 5–8] have extensively discussed the switching behaviour of AFLCs at field strength below \mathbf{E}_{th}^{AF-F} . In the applied field strength scale two major processes take place at $\mathbf{E} < \mathbf{E}_{th}^{AF-F}$: helix unwinding and Fréedericks transition.

3.1. Helix unwinding

For typical AFLCs, the director is arranged in a double helix, one for the even-numbered and another for the odd-numbered smectic layers, both having equal pitches. It was demonstrated in the resonant X-ray diffraction measurements of Mach *et al.* [12] that in AFLCs, the c -directors in the adjacent smectic layers, due to the chirality, are not exactly antiparallel to each other, i.e. $(\varphi_{i+1} - \varphi_i) \neq \pi$. As a consequence, the vectors of \mathbf{P}_s of the adjacent layers are also not antiparallel. This results in a non-zero local polarization, so called *residual polarization* [13]. In the absence of an applied electric field and surface stabilization, this polarization naturally spirals and is thus totally compensated in the AFLC material. An electric field applied perpendicular

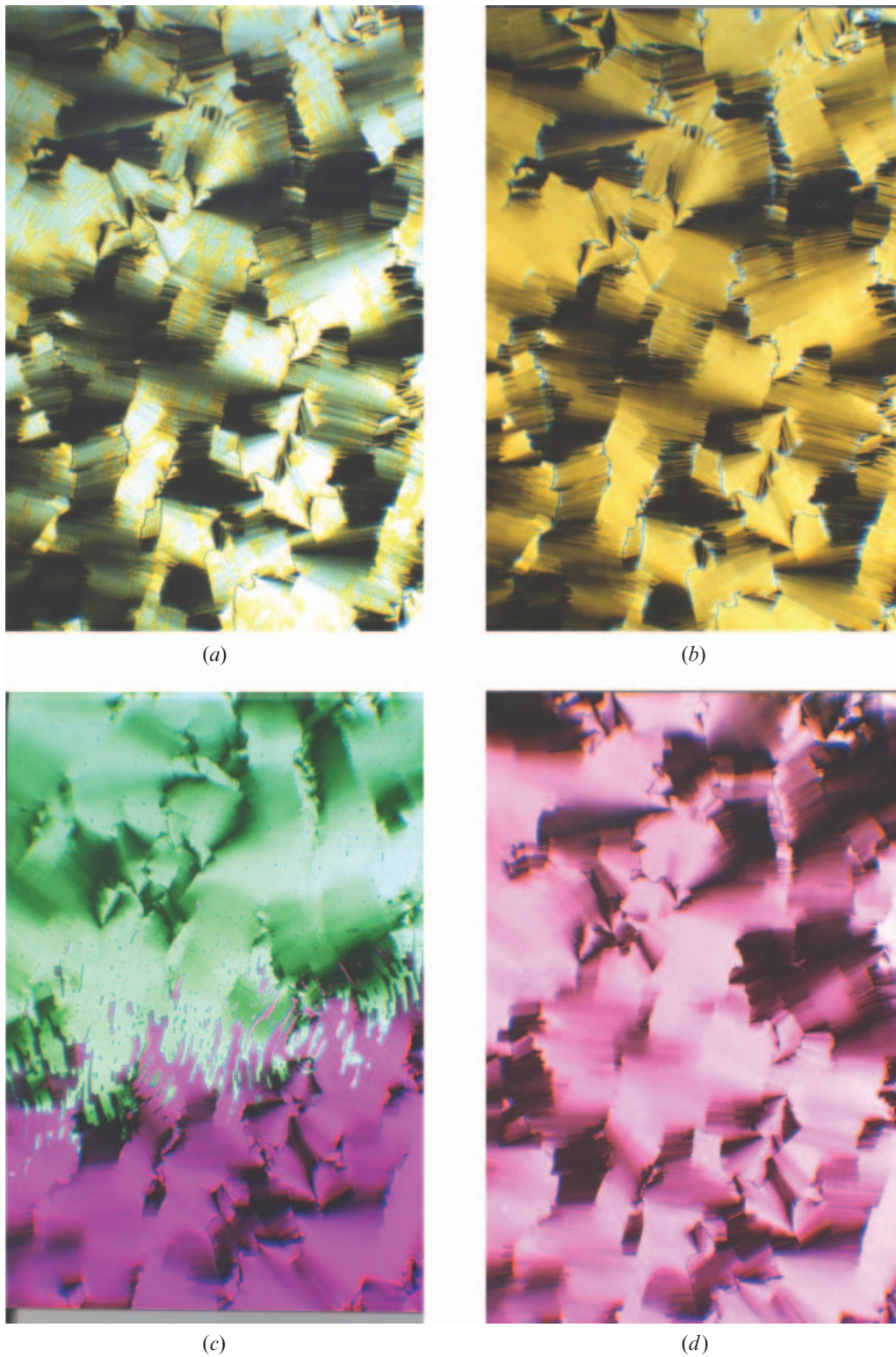


Figure 2. Photomicrographs of a non-uniformly aligned cell filled with di(4PPB5)3Si, (a) in the HAF state at $E=0$, (b) in the pretransitional region, (c) at the field-induced AF-F transition with the F state, the region at the bottom of the picture in red/pink, (d) in the field-induced F state.

to the smectic layer normal will couple to this residual polarization and, as a consequence, the helical molecular order will, with increasing field strength, be first distorted and then completely unwound. The helix distortion in this case would occur with a periodicity equal to that of the residual polarization which is one-pitch. This, however, is in contradiction with the recently presented simple model for field-driven helix unwinding in an AFLC [14], in which the applied electric field causes a perturbation in the anticlinic order that induces a polarization along the local direction of the c -directors. The field-induced polarization \mathbf{P}_{ind} then interacts with the applied electric field resulting in helix distortion with wavelength of half of a pitch in accordance with anticlinic symmetry of the AFLC.

The molecular helical order in AFLCs may be suppressed by interactions with the confining solid surfaces as mentioned above. Such a surface stabilization with strong planar anchoring will result in a

horizontal AF state (HAF) with the directors lying in the plane parallel to the confining substrates, as shown in figure 3. The obtained textures in most of our samples were recognized as being of the HAF type.

3.2. Fréedericks transition

As mentioned before, the applied electric field distorts the anticlinic molecular order in AFLCs. Qian and Taylor [3] pointed out that instead of a continuous variation of the director orientation with the field, a sharp transition, similar to the Fréedericks transition in nematics, takes place in the case of the HAF state at $\mathbf{E}_{\text{th}}^{\text{Fréed}}$ (Fréedericks threshold field). For $\mathbf{E} < \mathbf{E}_{\text{th}}^{\text{Fréed}}$ the director orientation profile is not disturbed, i.e. $\Delta\varphi = \pi$. However, on increasing the field strength above $\mathbf{E}_{\text{th}}^{\text{Fréed}}$, the molecules in adjacent layers undergo an unequal rotation resulting in a deviation from the perfect anticlinic order. Such a deviation is represented by $\alpha = \frac{1}{2}(\pi - \Delta\varphi)$ and gives rise to a local polarization \mathbf{P}_{ind} .

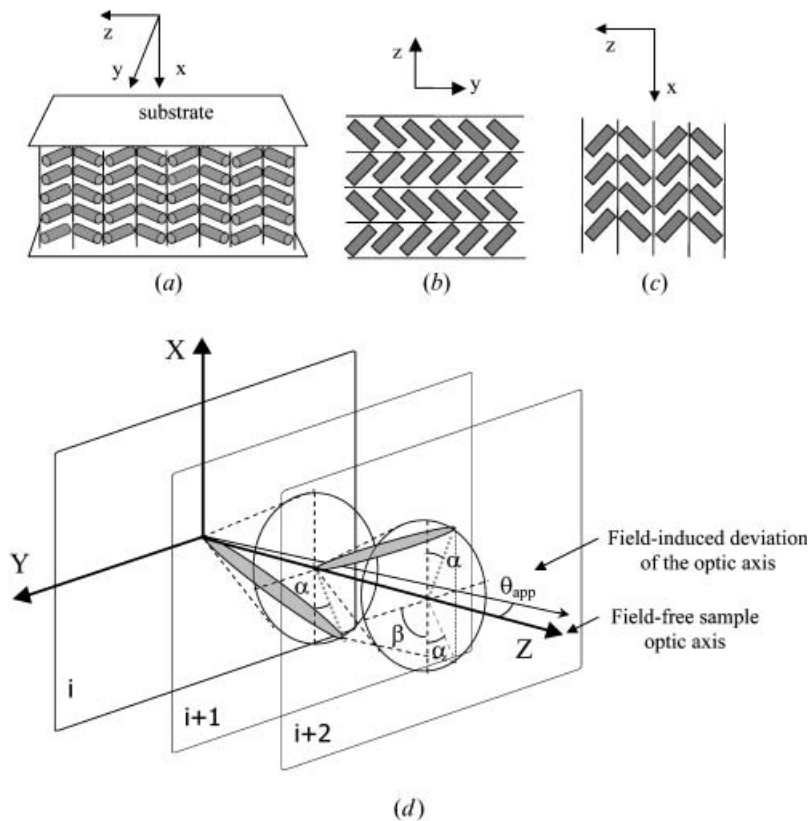


Figure 3. Schematic representation of an AFLC in a conventional sandwich cell aligned in: (a) and (b) horizontal AF (HAF) texture, before applying an electric field directed along the X -axis, (c) vertical AF (VAF) texture, after the Fréedericks transition under an applied electric field (note that the figure is a simplified picture of the AF molecular order, as there is no positional order). The transition from HAF to VAF state results in changed birefringence of the sample, $\Delta n_{\text{HAF}} < \Delta n_{\text{VAF}}$. (d) When the antiferroelectric order is distorted, i.e. $\Delta\varphi = \varphi_{i+1} - \varphi_i \neq \pi$, a field-induced in-plane deviation (tilt) θ_{app} of the sample optic axis takes place; α and β represent, respectively, the degree of deviation from the AF order and the rotation of the position of the AF pair with respect to that in the HAF state, respectively.

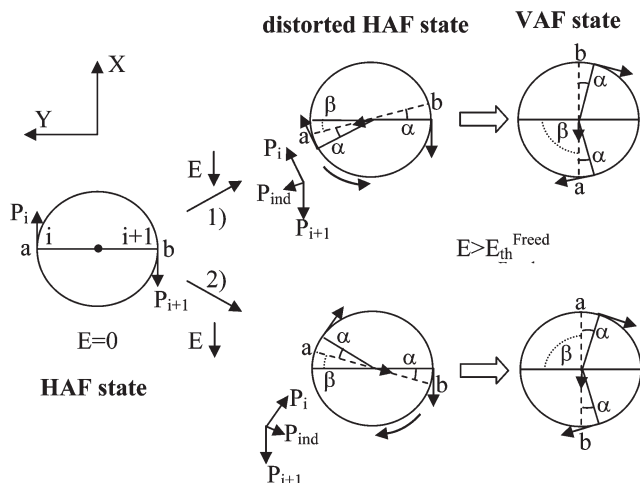


Figure 4. Schematic representation of the Fréedericks transition in an AFLC at different polarities of the applied electric field $E > E_{th}^{Freed}$. An electric field applied along the smectic layers of the HAF state, i.e. along the X -axis, distorts the perfect antiferroelectric order $\alpha=0$ [$\alpha = 1/2 (\pi - \Delta\varphi)$, where $\Delta\varphi = \varphi_{i+1} - \varphi_i \neq \pi$]. In the distorted HAF state there is a field-induced polarization P_{ind} oriented along the average c -director of the deformed anticlinic pair. The applied field orients P_{ind} along the field, thus the distorted HAF state transforms into a VAF state.

In figure 4 are presented schematically undistorted ($E=0$) and distorted ($E > E_{th}^{Freed}$) HAF states at different field polarity. The field-induced polarization P_{ind} is oriented along the average c -director of the distorted anticlinic pair. The applied electric field will tend to orient P_{ind} along the field, thus rotating the average c -director of the distorted anticlinic pair until it aligns along the field, resulting thus in a transformation of the HAF state to the vertical AF (VAF) state, the so-called Fréedericks transition that resembles the one in nematics [3]. It should be noted that the compounds studied in this work exhibited a high P_s . Therefore, a very small disturbance of the anticlinic order in these compounds, and thus of the condition for conciliation of P_s in the AFLC state, will lead to a field-induced polarization P_{ind} of substantial magnitude.

The Fréedericks transition in AFLCs, according to [3], is characterized by a threshold voltage $V_{th} = 2\pi (UK/P_s^2)^{1/2}$ which is thickness independent. This transition begins by an abrupt jump in the anticlinic order α followed by a continuous rotation of the anticlinic pair characterized by β , as shown in figure 4. A characteristic feature of the Fréedericks transition in AFLCs is that the perturbation of the anticlinic order α remains very small ($\alpha \ll \beta$) whereas the rotation angle of the anticlinic pair, given by β , towards the direction of the applied electric field tends to $\pi/2$ with increasing field

strength. A Fréedericks transition, i.e. the transformation from HAF to VAF state, will result in changes in the birefringence of the sample as well as in the tilt of the sample optic axis that will affect the intensity of transmitted light through the sample. As seen in figures 3 and 4, as the distortion of the anticlinic order α increases, the in-plane induced deviation θ_{app} of the sample optic axis increases.

The optical transmission I of a sample inserted between crossed polarizers is expressed by:

$$I = I_0 \sin^2(2\Psi + \theta_{app}) \sin^2\left(\frac{\pi d \Delta n}{\lambda}\right) \quad (4)$$

where I_0 is the light intensity through the sample when the polarizers are parallel and θ_{app} is the angle between the sample optic axis and the polarizer. Δn is the optical anisotropy of the sample and d is the cell gap thickness; λ is the wavelength of the incoming light. The optical properties of AFLCs are described by Elston *et al.* [15, 16] and de Meyere *et al.* [17]. During the switching from HAF to VAF state (Fréedericks transition) the birefringence of the sample changes from $\Delta n_{HAF} = (n_z - n_y)$ to $\Delta n_{VAF} = (n_z - n_x)$, where n_x , n_y and n_z are given by [15]:

$$\begin{aligned} n_x &= n_o \\ n_y &= (n_o^2 \cos^2 \theta + n_e^2 \sin^2 \theta)^{1/2} \\ n_z &= (n_o^2 \sin^2 \theta + n_e^2 \cos^2 \theta)^{1/2} \end{aligned} \quad (5)$$

where n_o and n_e are the ordinary and extraordinary refractive indices, respectively. Since for $\theta \leq 45^\circ$, $n_z \geq n_y > n_x$, thus $\Delta n_{HAF} < \Delta n_{VAF}$. This results in changes in the colour appearance of the sample. Moreover, due to the distortion of the anticlinic order, characterized by α in figure 3, there will be a field-induced deviation of the sample optic axis that previously, as argued in [15], was ascribed incorrectly to the *electroclinic* effect.

In figure 3 the field-induced in-plane deviation θ_{app} of the optic axis in AFLCs due to distortion of the anticlinic order is schematically presented. As seen, the larger α is (i.e. the larger the degree of distortion of the anticlinic order), the larger is the field-induced in-plane deviation θ_{app} of the sample optic axis. As we shall see, the perturbation of the anticlinic order α in some of our compounds is quite substantial, resulting in a significant field-induced in-plane deviation of the sample optic axis.

4. Results and discussion

Molecular tilt θ and P_s are important material parameters of FLCs and AFLCs. In many studies, however, the apparent optical tilt angle θ_{app} is used instead of θ .

Even though θ_{app} differs somewhat from θ defined by X-ray studies, the θ_{app} is a convenient parameter to study since it can easily be measured from the electro-optical response of the F phase. It is also a useful parameter for characterizing the electro-optical properties of AFLCs where the tilt direction alters its sign in adjacent layers. In the case of an AFLC, the molecular tilt θ could be considered, with a reasonable approximation, to be equal to the saturated value of θ_{app} measured in the field-induced F state [18]. In this study θ_{app} was measured as a half of the saturated switching cone angle in the field-induced F state that was found by rotating the sample between crossed polarizers and detecting the position of two consecutive minima in the transmitted light intensity. θ_{app} describes also, as we shall see, the field dependent tilt direction of the sample optic axis in the pretransitional region of the AF state. The temperature dependence of θ_{app} of the dimeric siloxanes is shown in figure 5(a). As can be

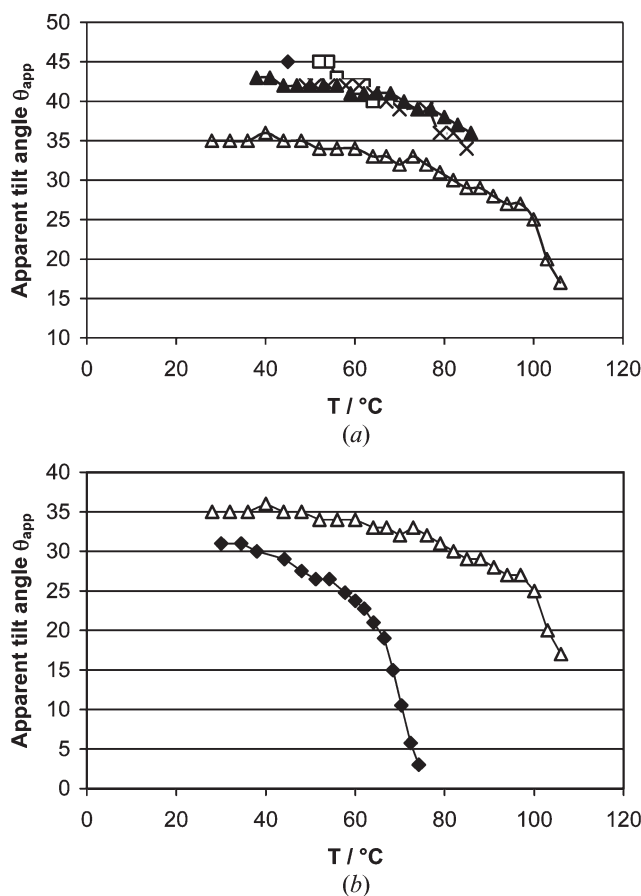


Figure 5. (a) Apparent tilt angles (deg.) of the siloxane dimers di(4PPB m)3Si as a function of temperature: $m=3$ (\blacklozenge); $m=4$ (\square); $m=5$ (\times); $m=6$ (\blacktriangle); $m=11$ (\triangle). (b) Apparent tilt angles of the dimer with $m=11$ (\triangle) compared with the corresponding monomer (\blacklozenge).

seen, the compounds studied in this work exhibit a large θ_{app} whose saturated values in the field-induced F state are within the range of 36° – 45° . Compared with its corresponding monomer, θ_{app} of the dimer is larger and less temperature-dependent. This is illustrated in figure 5(b) for di(4PPB11)3Si. The di(4PPB3)3Si and di(4PPB4)3Si compounds showed the largest value of θ_{app} , 45° , or very near to this value. In di(4PPB5)3Si and di(4PPB6)3Si θ_{app} was measured close to 45° over a broad temperature range with weak temperature dependence. Except for di(4PPB11)3Si, all the compounds, when aligned in HAF texture with smectic layers perpendicular to the confining substrates and with tilt plane parallel to the substrates, exhibited field-free *black* state with very low in-plane birefringence ($\Delta n \approx 0$) corresponding to a state with almost isotropic optical properties [18]. The large value of θ_{app} makes these materials very attractive for applications in displays and photonic devices.

The P_s of the field-induced F state is the other important material parameter of AFLCs. Except for di(4PPB3)3Si the dimers showed large P_s values which at low temperatures were in the range 250 – 300 nC cm $^{-2}$, as shown in figure 6. As can be seen, the P_s of these materials exhibited a peculiar linear temperature dependence, which is quite rare among FLCs. Figure 6 also shows that the P_s of the dimers is lower than that of their corresponding monomer. The P_s of di(4PPB3)3Si could not be measured properly since the electric field induced a more ordered phase in the material during the measurements.

An AF–F transition has been found to take place in the compounds under study when the applied electric field E exceeded a certain threshold value $E_{\text{th}}^{\text{AF–F}}$ specific for each compound. In figure 7 the temperature

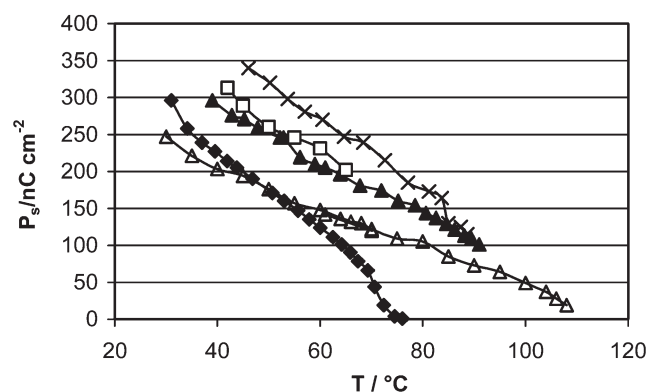


Figure 6. Polarization in the field-induced F state measured as a function of temperature for the siloxane dimers di(4PPB m)3Si with $m=5$, 6 and 11 carbons in the bridging chains, compared with the 11-monomer without siloxane: $m=4$ (\square); $m=5$ (\times); $m=6$ (\blacktriangle); $m=11$ (\triangle); 11-monomer (\blacklozenge).

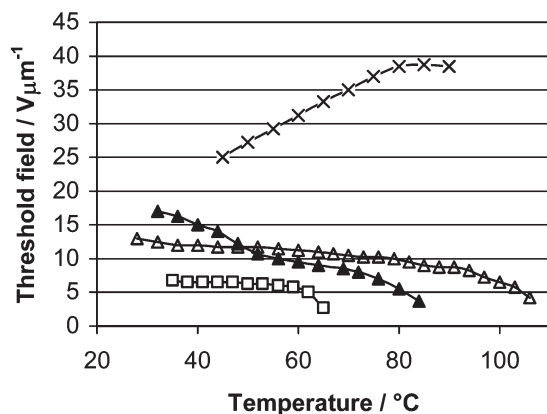


Figure 7. Temperature dependence of the Fréedericks threshold field E_{th}^{AF-F} for the siloxane dimers $di(4PPBm)3Si$: $m=4$ (\square); $m=5$ (\times); $m=6$ (\blacktriangle); $m=11$ (\triangle).

dependence of E_{th}^{AF-F} is plotted for the $(4PPBm)3Si$ with $m=4, 5, 6$ and 11 . Initially the value of E_{th}^{AF-F} for the $di(4PPB4)3Si$ and $di(4PPB11)3Si$ compounds increased rapidly with decreasing temperature before achieving a saturation, whereas E_{th}^{AF-F} of $di(4PPB5)3Si$ showed the reverse behaviour, i.e. decreased continuously on cooling. The temperature dependence of $di(4PPB6)3Si$ showed an S-shaped form, with an inflection point at the temperature $T_{tr} \approx 60^\circ C$. As will be shown later, T_{tr} is the temperature at which the field-induced AF-F transition for this compound on cooling started a transformation from first order to a continuous transition (i.e. of second order) over a $15^\circ C$ temperature range down to about $45^\circ C$.

The AF coupling coefficient U of the dimeric siloxanes was derived from equation (2) and is plotted in figure 8 as a function of temperature. The coefficient U has the highest value for $di(4PPB5)3Si$, which also in

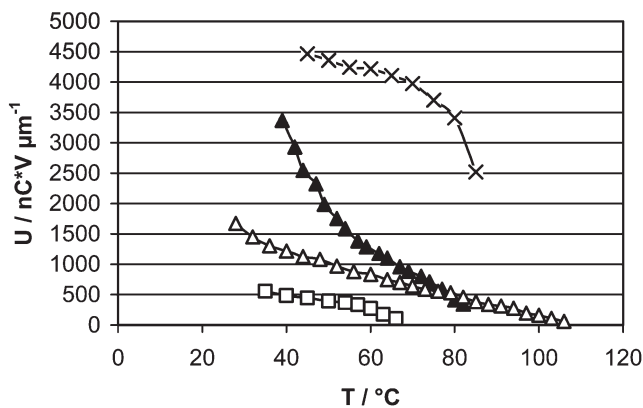


Figure 8. Temperature dependence of the AF coupling coefficient U of the siloxane dimers $di(4PPBm)3Si$: $m=4$ (\square); $m=5$ (\times); $m=6$ (\blacktriangle); $m=11$ (\triangle).

contrast to the other dimers shows saturation of U with decreasing temperature. However, for $di(4PPB4)3Si$ and $di(4PPB11)3Si$ much lower values were found, which increased continuously on lowering the temperature. The temperature dependence of U found for $di(4PPB6)3Si$, however, was found to be quite different from that of the other siloxane dimers. It showed two distinct rates of increase of U on lowering the temperature. The change in rate, as seen in figure 8, took place at the same temperature T_{tr} mentioned above.

The behaviour of the field-induced AF-F transition observed in $di(4PPB6)3Si$ is of particular interest. In figure 9 the appearance of this AF-F transition at different temperatures is depicted in a photomicrograph sequence. At temperatures higher than $T_{tr} \approx 60^\circ C$, the field-induced transition from AF to F is sharp, manifested by the propagation of quasi-one-dimensional

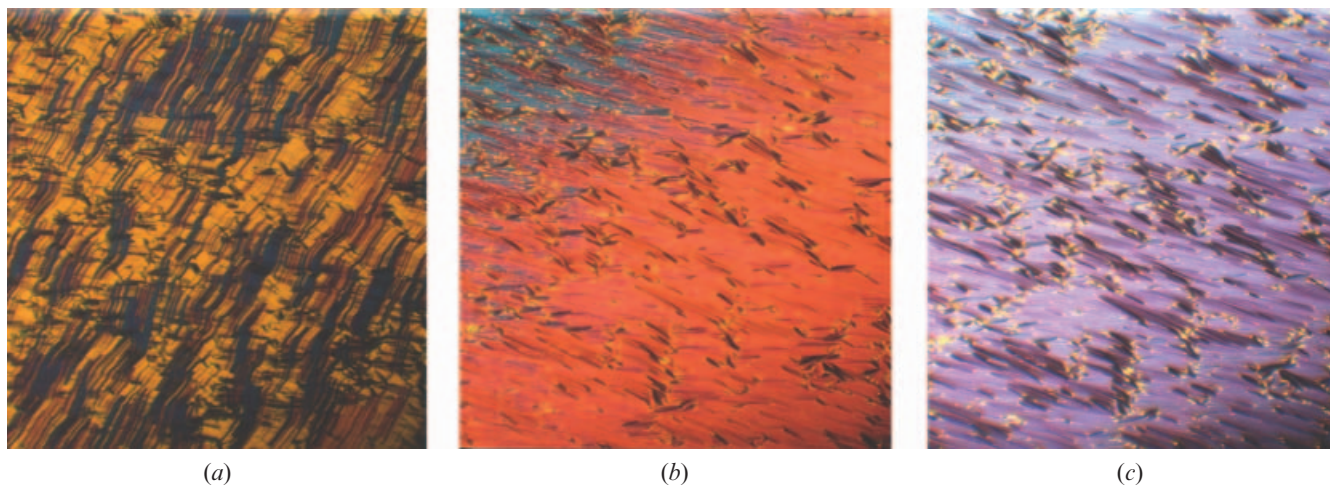


Figure 9. Field-induced AF-F transition of the siloxane dimer $di(4PPB6)3Si$ at (a) $80^\circ C$, (b) $50^\circ C$ and (c) $40^\circ C$.

finger-like solitary waves along the smectic layers. As mentioned, the generation and propagation of finger like solitary waves indicates a field-induced AF–F transition of first order. On approaching the temperature T_{tr} , however, the AF–F transition gradually changed its character: the fingers of synclinic (F) order, invading the regions with anticlinic (AF) order, became increasingly less pronounced and smaller. On decreasing the temperature below T_{tr} , the F state started to emerge in the AF state in the form of a set of domains, whose size continuously grew with the applied electric field. The AF–F transition in these domains occurred in the form of propagating solitary waves with less distinct edges than is usually the case. The field-induced tilt of the sample optic axis in the pretransitional region of the AF state, and thus the birefringence, increased with decreasing temperature which means that the actual AF–F transition also became increasingly less pronounced. This process was also accompanied by a continuous increase of nucleation points for the AF–F transition. Hence, the character of the field-induced AF–F transition continuously changed from first to second order on lowering the temperature. At temperatures below $T \approx 45^\circ\text{C}$, the AF–F transition in di(4PPB6)3Si was found to be continuous. This

behaviour is illustrated in figures 9(b) and 9(c). The transformation of the AF–F transition from first to second order in di(4PPB6)3Si, as found experimentally in this work, was completed in a temperature interval of about 15°C .

Another way to investigate the field-induced AF–F transition is to study the hysteresis of the transition. It was mentioned already that whether the field-induced AF–F transition will be of first or second order depends on the relative height of the free energy barrier, J , separating the F and AF states. According to [3, 19] for a small energy barrier J , the field-induced AF–F transition becomes second order, i.e. the anticlinic molecular order transforms continuously into synclinic when the field strength is increased. The first order AF–F transition becomes second order at $J = U/10$ [3]. Parry-Jones and Elston [19] demonstrated that at $J = U/20$ the electro-optic response due to the field-induced AF–F transition has a ‘V-shaped’ form indicating continuous change from AF to F state, a kind of switching that may be related to a thresholdless AF–F transition. On the other hand, when $J = U/5$, the electro-optic response exhibits a distinct hysteresis characteristic for first order AF–F transitions. The AF–F transition takes place at E_{th}^{AF-F} whereas the field-induced F state relaxes to the

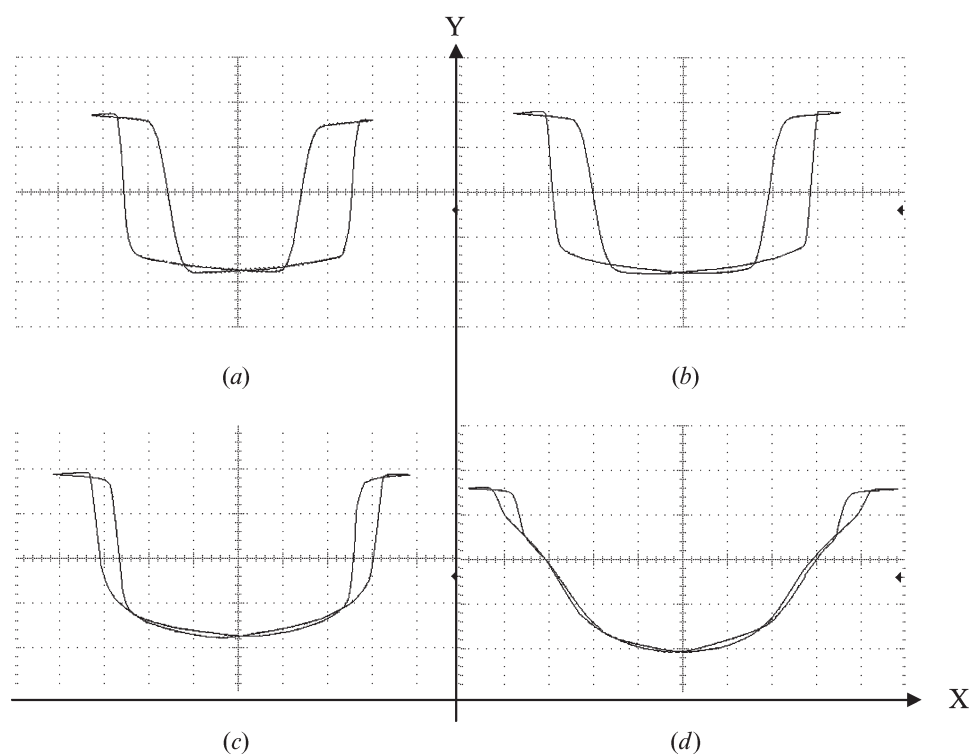


Figure 10. Electro-optic response of the siloxane dimer di(4PPB6)3Si at (a) 75°C , (b) 65°C , (c) 55°C and (d) 45°C . The oscilloscope pictures have been digitally enhanced to facilitate reading. The Y-axes represent the optical intensity in arbitrary units and the X-axis the field, each scale bar representing 5 V.

field-free AF state at E_{th}^{F-AF} . The fact that $E_{th}^{AF-F} > E_{th}^{F-AF}$ indicates a presence of hysteresis. Figure 10 shows a series of electro-optic response curves for di(4PPB6)3Si at different temperatures. The response for temperatures above T_{tr} exhibits a distinct hysteresis; hence, the field-induced AF-F transition in this temperature range should be considered as of first order. It can be seen that on approaching T_{tr} from above, the difference between E_{th}^{AF-F} and E_{th}^{F-AF} gradually decreases, and below $T=45^\circ\text{C}$ becomes very close to zero, indicating that the AF-F transition is now of second order. The electro-optic response curve in the temperature region below T_{tr} adopted mixed U/V shape that at $T=45^\circ\text{C}$ resembles very much that seen in the case of thresholdless antiferroelectricity. Hence, depending on temperature, the field-induced AF-F transition in di(4PPB6)3Si is either of first or second order. As seen in figure 8, such a change in the character of the AF-F transition coincides with the rapid increase of U with decreasing temperature below T_{tr} and thus with a probable decrease of the ratio J/U . This in turn results in a change in the character of the field-induced AF-F transition from first to second order. This is, to the best of our knowledge, the first example of transformation of the order of this transition with temperature.

Diminishing the difference between E_{th}^{AF-F} and E_{th}^{F-AF} on lowering the temperature was also found in di(4PPB11)3Si. However, before this difference became zero, i.e. before the field-induced AF-F transition changed its character fully from first to second order, the material crystallized. All the other compounds, the dimers with $m=3, 4$ or 5 , exhibited only a first order field-induced AF-F transition, manifested by a distinct electro-optic hysteresis loop as well as by the generation and propagation of finger-like solitary waves.

Another peculiarity in the behaviour of di(4PPB6)3Si that could be regarded as a strong indication for the transformation of the field-induced AF-F transition from first to second order, is the sharp change in the relaxation time of the AF state from the field-induced F state. The decay time τ_d of the electro-optic response due to the AF-F transition was used as a measure of τ_r for the substances studied in this work, i.e. $\tau_d \sim \tau_r$.

Figure 11 shows the temperature dependence of the relaxation times τ_r of the cells containing di(4PPB m)3Si with $m=4, 5, 6$ and 11 . An electric field with a unipolar square wave of period 10 Hz was applied to the cell. The temperature behaviour of γ was evaluated from the temperature dependence of the switching time in the field-induced F state given by $\tau_{SmC} = \gamma/PE$. It is reasonable to assume that the elastic constant K equation (3), undergoes no drastic change at the peculiar temperature

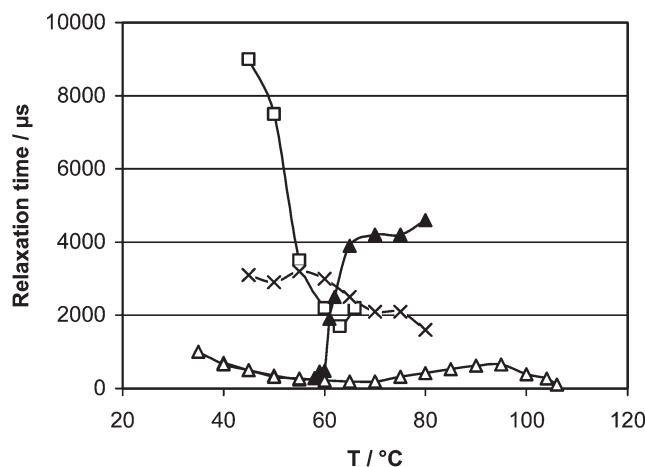


Figure 11. Relaxation times of the AF state from the field-induced F state for siloxane dimers di(4PPB m)3Si: $m=4$ (\square); $m=5$ (\times); $m=6$ (\blacktriangle); $m=11$ (\triangle).

T_{tr} . As seen from figure 11, τ_r found in the compound with $m=6$, unlike the other compounds in the present study, decreased sharply on approaching the temperature T_{tr} from above. However, no substantial changes of τ_{SmC}^* , and thus of γ , were found to take place in a wide temperature region centred at T_{tr} , in this compound. On the other hand, as mentioned above, the slope of the temperature dependence of U increased at T_{tr} on lowering the temperature. Such a change of slope was attributed to the transformation of the AF-F transition from first to second order. However, the temperature behaviour of U could not explain such a sharp reduction of τ_r found in di(4PPB6)3Si. There must be another reason.

As already mentioned, when decreasing the temperature below T_{tr} , the field-induced AF-F transition no longer occurs in the form of continuously propagating finger-like solitary waves. The transition texture just below T_{tr} , i.e. in the transient region where the transformation of the AF-F transition from first to second order is incomplete, appeared in the form of a domain-like pattern. The same is valid for the F-AF transition. As a consequence of that, the retreating fingers of the AF state in the domain-like pattern have a much smaller distance to cover (equal to the size of the domain), compared with the F-AF transition at temperatures higher than T_{tr} , and hence the τ_r time will be much shorter. Consequently, the sharp reduction of τ_r on lowering the temperature could also be considered as an indication of the transformation of the AF-F transition from first to second order. Most important, the detected short τ_r at temperatures below T_r indicates a substantial reduction of J which, as mentioned above, is the reason for hysteresis-free electro-optic response at these temperatures.

AFLC compounds with tilt approaching 45° are considered to be very attractive for achieving a high quality field-free dark state and thus high contrast AFLC displays [17, 18, 20]. It should be noted that the long relaxation time τ_r of the transition from field-induced F state to field-free AF state of AFLC compounds with first order field-induced AF–F transition, is probably one of the main obstacles for utilizing AFLC compounds with a molecular tilt of 45° in displays. As was found in this study, as well as in previous studies, such compounds exhibit the coexistence of AF and F states, which considerably diminishes the contrast of the AFLCDs [21, 22] and renders these compounds inappropriate for display applications. Hence, the high molecular tilt of the AFLC of about 45° is a necessary but insufficient condition for obtaining high performance AFLCDs. As this study showed, AFLCs with tilt angle approaching 45° could

be appropriate for use in LCDs if the field-induced AF–F transition is *thresholdless*, i.e. of second order [19], such as exhibited by di(4PPB6)3Si.

Field-induced changes of both Δn and θ_{app} were found to take place in the compounds studied in this work. The character of these changes varied from one substance to another. For instance, in di(4PPB3)3Si it was found that in the pretransitional region (as seen from the photomicrographs of a sample containing this compound presented in figure 12), there is no detectable field-induced tilt of the optic axis at $\mathbf{E} < \mathbf{E}_{\text{th}}^{\text{AF-F}}$. Indeed, on examining the behaviour of the circular domain marked in figure 12(b) it can be seen that only the interference colour of this domain changes when applying an electric field in the interval $0 < \mathbf{E} \leq \mathbf{E}_{\text{th}}^{\text{AF-F}}$, which indicates a field-induced transition from HAF to VAF state. The position of the black cross in the domains is not changed by the applied field, indicating

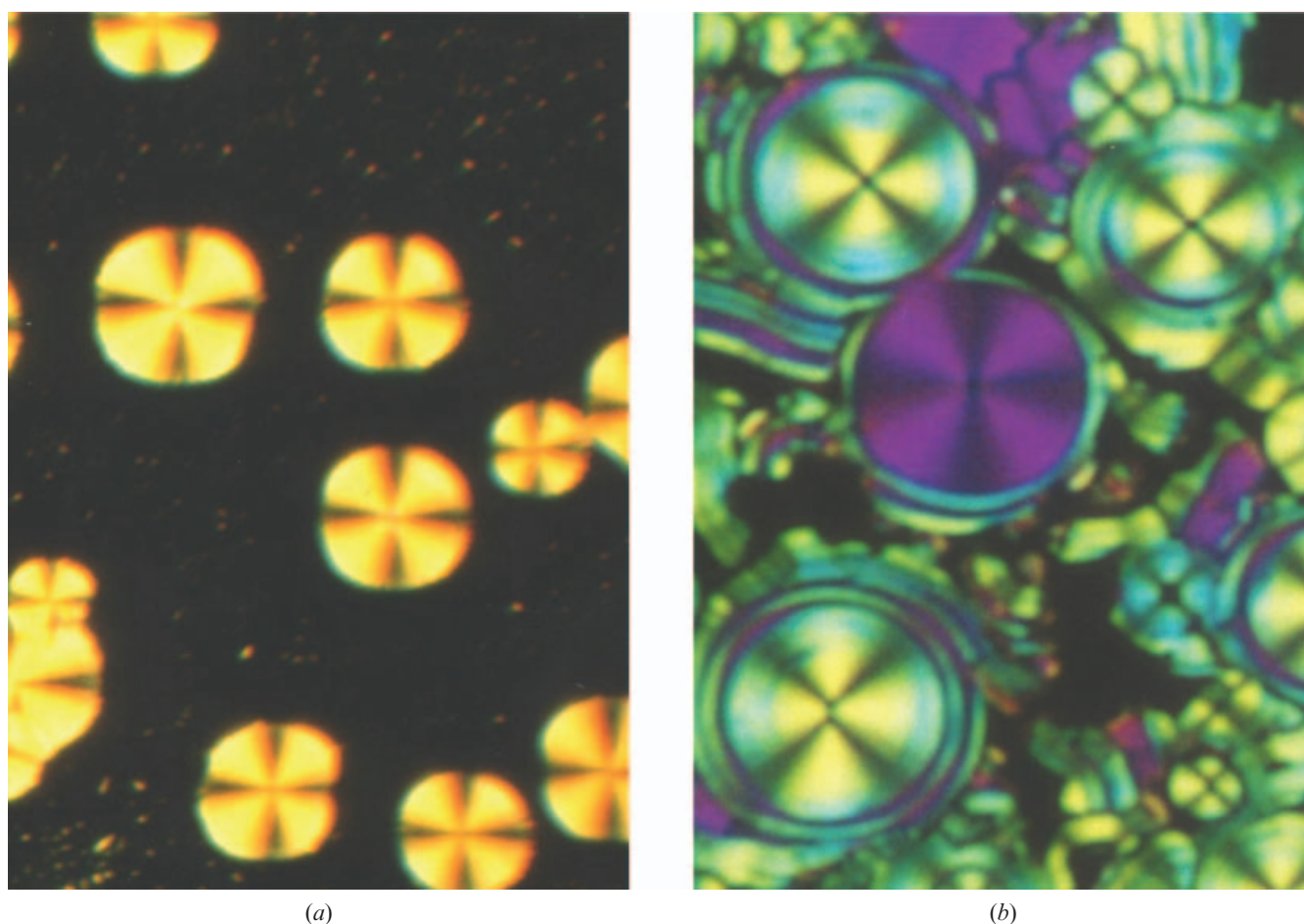


Figure 12. Photomicrographs of the texture of di(4PPB3)3Si: (a) without field and (b) at the AF–F transition. Note the birefringence change of the circular domains in the AF state from yellow to purple due to the Fréedicks transition, i.e. due to the field-induced transition from HAF to VAF state that takes place with no significant change of the position of the cross. This indicates that there is no significant change in the position of the sample optical axis during the transition. The green domains are in the field-induced F state.

that the position of the sample optic axis remains almost parallel to the smectic layers normal. Hence, below the field-induced AF–F transition, the distortion of the anticlinic order α in this compound must be very small indeed. In other words, the field-induced AF–F transition in di(4PPB3)3Si is very sharp, with almost zero field-induced tilt of the sample optic axis.

The other dimers, however, displayed a quite different behaviour, di(4PPB5)3Si for instance. The electro-optic response of this compound at different field strengths is given in figure 2. Following the changes in the interference colour of the sample at a certain temperature, as well as in the position of the black line on a chosen focal-conic domain (which in fact represents a part of the cross of a circular domain), it could be concluded that the changes of both Δn (colour changes) and θ_{app} (field-induced in-plane deviation of the local optic axis) take place in the sample before a sharp AF–F transition occurs at this temperature. Such changes of Δn and of the in-plane position of the optic axis, i.e. of θ_{app} , will affect the transmission characteristics of the sample, as follows from equation (4). This can be clearly seen in figure 10, showing the electro-optic response of di(4PPB6)3Si. In this work, however, only the field-induced tilt of the optic axis of dimeric siloxanes in the pretransitional region was investigated. From the detected pretransitional behaviour of the siloxane dimers with $m=4, 5, 6$ and 11 , we may conclude that the VAF state (with $\beta=\pi/2$) in these compounds has strongly distorted AF order, i.e. with large α .

Figures 13, 14 and 15 show the field dependence of the field-induced in-plane deviation of the sample optic axis θ_{app} for di(4PPB5)3Si, di(4PPB6)3Si and di(4PPB11)3Si, respectively, at $E < E_{th}^{AF-F}$, i.e. in the pre-transitional (Fréedericks transition) region; as well

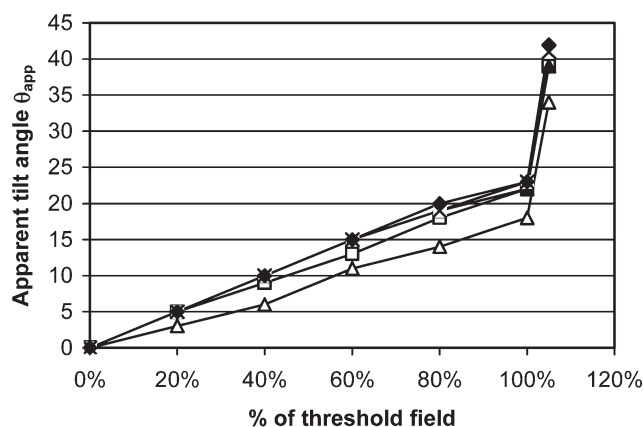


Figure 13. Field-induced tilt of the sample optic axis θ_{app} of di(4PPB5)3Si as a function of temperature: 51°C (\blacklozenge); 64°C (\times); 70°C (\blacktriangle); 76°C (\square); 85°C (\triangle).

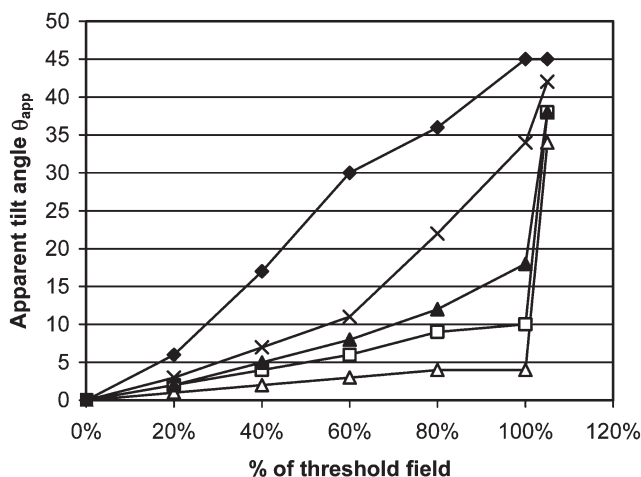


Figure 14. Field-induced tilt of the sample optic axis θ_{app} of di(4PPB6)3Si as a function of temperature: 40°C (\blacklozenge); 50°C (\times); 60°C (\blacktriangle); 70°C (\square); 80°C (\triangle).

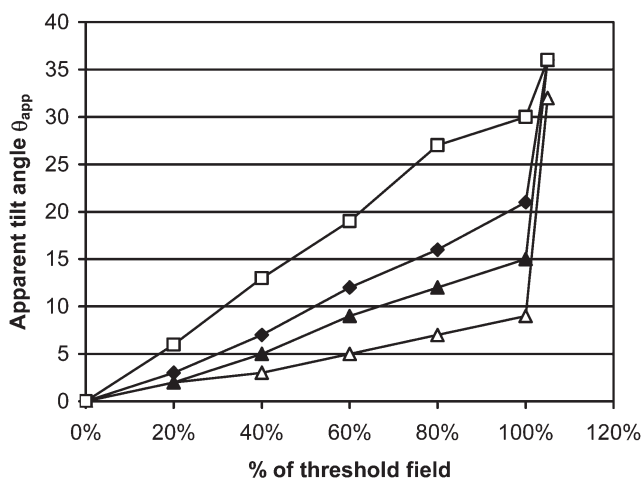


Figure 15. Field-induced tilt of the sample optic axis θ_{app} of di(4PPB11)3Si as a function of temperature: 30°C (\square); 50°C (\blacklozenge); 70°C (\blacktriangle); 90°C (\triangle).

as the apparent tilt θ_{app} , at $E > E_{th}^{AF-F}$, i.e. in the field-induced F state, at different temperatures. For these compounds, in broad temperature regions (except the temperature region of di(4PPB6)3Si where the field-induced AF–F transition is of second order), an almost linear dependence of the induced in-plane deviation θ_{app} of the sample optic axis on the applied electric field was found. As can be seen in figure 16, the maximum values of θ_{app} are quite similar for di(4PPB5)3Si, di(4PPB6)3Si (at $T > T_{tr}$) and di(4PPB11)3Si, whereas those measured in di(4PPB4)3Si are much lower. Such large value of θ_{app} in the pre-transitional region of an AFLC such as that found in di(4PPB5)3Si were reported in [23, 24]. An estimation made for di(4PPB5)3Si and di(4PPB6)3Si, exhibiting molecular tilt close to 45°, shows that the

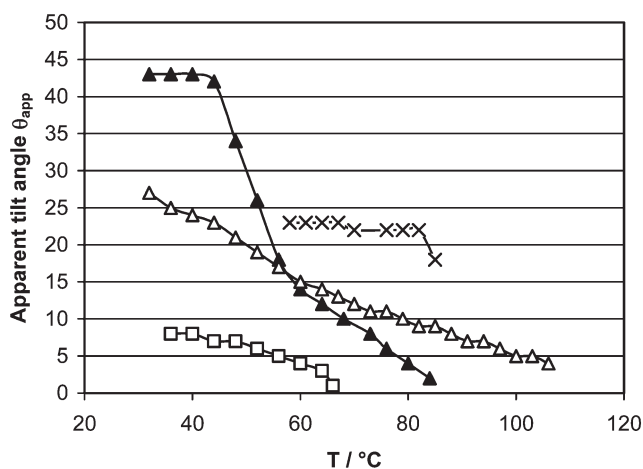


Figure 16. Temperature dependence of the maximum apparent tilt in the pretransitional region of the dimers: $m=4$ (□); $m=5$ (×); $m=6$ (▲); $m=11$ (Δ). It should be noted that when approaching a continuous transition and the maximum pretransitional apparent tilt angle increases, the AF–F transition becomes less defined and the values measured more uncertain, so that figure 13–15 give a more complete view of the behaviour of each compound.

measured field-induced tilt θ_{app} of 20° – 23° corresponds to a distortion of the AF order α of about 30° . For di(4PPB11)3Si α was estimated to be even larger. Hence, it can be concluded that the flexibility of the chains bridging the mesogens into a dimeric structure allows a substantial deformation of the anticlinic molecular order in these compounds by the applied electric field without triggering AF–F transition.

The field-induced tilt θ_{app} of di(4PPB6)3Si, in the temperature region where the field-induced AF–F transition is predominantly of second order, showed a non-linear dependence on the applied electric field. θ_{app} increased faster and continuously with the field strength compared with the field-dependence of θ_{app} found in the higher temperature region of this material, where the field-induced AF–F transition is of first order. In the case of di(4PPB4)3Si, di(4PPB5)3Si and di(4PPB11)3Si, as shown in figure 16, the maximum value of induced tilt θ_{app} , as a function of temperature, general increases with decreasing temperature, and in the cases of di(4PPB4)3Si and di(4PPB5)3Si, becomes saturated. Another quite peculiar temperature behaviour of θ_{app} , was found in di(4PPB6)3Si. On lowering the temperature below T_r , the temperature at which the transformation of the field-induced AF–F transition from first to second order begins, the maximum induced tilt θ_{app} increased abruptly. That might be regarded also as another indication for the beginning of the transformation of the field-induced AF–F transition from first to second order. The reasons for this behaviour, however, are not clear at present.

5. Conclusions

The bi-mesogenic siloxanes, di(4PPB m)3Si, with a carbon spacer length $m=4, 5, 6$ and 11 , studied in this work were found to exhibit an AF phase in a broad temperature interval that, in the case of di(4PPB6)3Si, also included room temperature. The field-induced F state of these compounds is characterized by large saturated apparent tilt θ_{app} (in the range 35° – 45°) and high spontaneous polarization P_s (in the range 250 – 350 nC cm $^{-2}$). All the compounds, except di(4PPB6)3Si and di(4PPB11)3Si in its lower temperature range, exhibited a field-induced AF–F transition of first order, manifested by the generation of finger-like solitary waves propagating along the smectic layers. The behaviour of the dimers with $m=4, 5, 6$ and 11 in the pre-transitional region, indicated a substantial flexibility of the chains bridging the mesogens into dimeric structure, allowing a large distortion of the AF molecular order by the applied electric field without triggering AF–F transition. The degree of flexibility seems to increase with the number m of the dimer. The peculiar temperature behaviour of di(4PPB6)3Si is of particular interest. It was found that below a certain temperature T_{tr} , the field-induced AF–F transition in di(4PPB6)3Si was gradually transformed from first to second order over a temperature range of about 15° . Several indications for this transformation were found. Firstly, the field-induced AF–F transition was no longer manifested by propagation of solitary finger-like waves. Instead, the field-induced F state emerged in the AF phase as randomly distributed spots, continuously growing in size with increasing applied electric field, with a colour different from that of the surrounding AF regions. Secondly, over the same temperature range from T_r to 15° below T_r , the electro-optic response curve gradually lost its hysteresis character, thus indicating a continuous field-induced AF–F transition which was also seen in the increase of the pre-transitional tilt, up to the point where a defined field-induced AF–F transition was no longer distinguishable and there was only a continuous colour change in the sample with increasing field strength. Thirdly, the slope of the temperature dependence of the antiferroelectric coefficient U increased substantially for temperatures below T_{tr} . Fourthly, the relaxation time τ_r of the AF state on removal of the applied electric field also exhibited a sharp reduction on lowering the temperature below T_{tr} .

An important finding in this work is that the relaxation time τ_r of the AF state from the field-induced F state is much shorter if the field-induced AF–F transition is of second order, and that the domains with second order transition that start to form at T_r seem to

be the reason for the sudden reduction of the relaxation time of the cell. One possible explanation for the transformation of the AF–F transition from first to second order is the substantial increase of the coefficient U on lowering the temperature below T_{tr} that possibly resulted in changes in the ratio J/U . However, the reason or reasons for such a transformation are not yet clear. Another possible reason could be certain conformational changes in the chains as well as in the siloxane unit connecting the two mesogenic groups, which might take place at temperatures below T_{tr} . The length of the chain bridging the mesogens into dimeric structure seems to play a very important role in the width of the pre-transitional region, the magnitude of θ_{app} , and in the appearance of a AF–F second order transition.

The pretransitional behaviour of the di(4PPB m)3Si compounds, where $m=4, 5, 6$ and 11 , was characterized by changes of both Δn and a large-induced tilt θ_{app} of the sample optic axis, whereas di(4PPB3)3Si exhibited changes of Δn only. The AFLC dimers exhibiting a large molecular tilt close to 45° and field-induced AF–F transition of second order have grey scale capability and a potential for displaying high contrast images, making these materials very attractive for application in displays and other liquid crystal devices.

Acknowledgements

The authors are indebted to C. Rosenblatt and P.L. Taylor for useful discussions. This work was supported by the Swedish Research Council and the Swedish Foundation for Strategic Research (SSF).

References

- [1] A.D.L. Chandani, E. Gorecka, Y. Ouchi, H. Takezoe, A. Fukuda. *Jpn. J. appl. Phys.*, **28**, L1265 (1989).
- [2] A.D.L. Chandani, T. Hagiwara, Y. Suzuki, Y. Ouchi, H. Takezoe, A. Fukuda. *Jpn. J. appl. Phys.*, **27**, L729 (1988).
- [3] T. Qian, P.L. Taylor. *Phys. Rev. E*, **60**, 2978 (1999).
- [4] J.-F. Li, X.-Y. Wang, E. Kangas, P.L. Taylor, C. Rosenblatt, Y.-I. Suzuki, P.E. Cladis. *Phys. Rev. B*, **52**, R13075 (1995).
- [5] B. Wen, S. Zhang, S.S. Keast, M.E. Neubert, P.L. Taylor, C. Rosenblatt. *Phys. Rev. E*, **62**, 8152 (2000).
- [6] S. Zhang, B. Wen, S.S. Keast, M.E. Neubert, P.L. Taylor, C. Rosenblatt. *Phys. Lett.*, **84**, 4140 (2000).
- [7] N.J. Mottram, R. Beccherelli, S.J. Elston. *Mol. Cryst. liq. Cryst. Sci. Technol., A*, **328**, 65 (1999).
- [8] L.A. Parry-Jones, S.J. Elston. *Ferroelectrics*, **276**, 267 (2002).
- [9] N. Olsson, B. Helgee, G. Andersson, L. Komitov. *Liq. Cryst.* (submitted).
- [10] H. Diamant, K. Drenk, R. Pepinsky. *Rev. sci. Instr.*, **28**, 30 (1957).
- [11] W.K. Robinson, C. Carboni, P. Kloess, S.P. Perkins, H.J. Coles. *Liq. Cryst.*, **25**, 301 (1998).
- [12] P. Mach, R. Pindak, A.M. Levelut, P. Barois, H.T. Nguyen, C.C. Huang, L. Furenliid. *Phys. Rev. Lett.*, **81**, 1015 (1998).
- [13] M. Buivydas, F. Gouda, G. Andersson, S. Lagerwall, B. Stebler. *Liq. Cryst.*, **23**, 723 (1997).
- [14] L.A. Parry-Jones, S.J. Elston. *Phys. Rev. E*, **63**, 050701 (2001).
- [15] R. Beccherelli, S.J. Elston. *Liq. Cryst.*, **25**, 573 (1998).
- [16] D.C. Ulrich, S.J. Elston. "The Optics of Thermotropic Liquid Crystals", S.J. Elston, R. Sambles (Eds), Taylor&Francis (1998).
- [17] A. de Meyere, J. Fournier, H. Pauwels. *Ferroelectrics*, **181**, 1 (1996).
- [18] N. Olsson, I. Dahl, B. Helgee, L. Komitov. *Liq. Cryst.*, **31**, 1555 (2004).
- [19] L.A. Parry-Jones, S.J. Elston. *Appl. Phys. Lett.*, **79**, 2097 (2001).
- [20] K. D'Have, A. Dahlgren, P. Rudquist, J.P.F. Lagerwall, G. Andersson, M. Matuszczyk, S.T. Lagerwall, R. Dabrowski, W. Drzewinski. *Ferroelectrics*, **244**, 115 (2000).
- [21] H. Coles. Private communication (1999).
- [22] P. Rudquist, K. D'Have, S.T. Lagerwall, R. Dabrowski. *ILCC'04*, July 4–9, 2004, Ljubljana, Slovenia, Poster APPL-P117.